The 2022 World Congress on
Advances in Civil, Environmental, & Materials Research (ACEM22)
16-19, August, 2022, GECE, Seoul, Korea

Dynamic behavior of shore connection of submerged floating tunnel under dynamic load

*Seok-Jun Kang[1)] and Gye-Chun Cho[2)]

[1), 2)] *Department of Civil and Environmental Engineering, KAIST, Daejeon 305-600, Korea*
[1)] *incheon@kaist.ac.kr*
[2)] *gyechun@kaist.edu*

ABSTRACT

A submerged floating tunnel (SFT) is designed to have buoyancy and is stabilized by tethers or pontoons to float in the water. Unlike tunnels installed underground, SFT is not constrained in all sections, so it behaves dynamically according to the wave load that is continuously applied. In the part where the SFT is connected to the shore, there is a risk of stress concentration at the connection because the constraint conditions in the underwater and underground sections are significantly different. In this study, the dynamic response of the shore connection of SFT in cyclic loading conditions was analyzed through a three-dimensional numerical analysis to examine the stability of the shore connection under the dynamic load condition. Considering the nonlinear characteristics of the ground, whose property changes according to the effective stress and strain level, the ground around the shore connection can be adequately simulated for the dynamic behavior. Furthermore, the stress and displacement occurring in the connection and the surrounding ground were evaluated according to the type of shore connection and the surrounding ground characteristics. As a result, it was confirmed that an appropriate level of flexible connection, not the rigid connection of a general tunnel, effectively secures dynamic stability.

1. INTRODUCTION

To cross the sea, it is necessary to utilize a special means of transportation or a route connecting the continents. Representative methods providing a path above sea level include transportation means such as airplanes or ships and providing pathways through bridges. However, these methods have limitations in that they are greatly affected by weather conditions or the distance between land. As an alternative, methods of constructing a tunnel under the seabed or immerging a tunnel on the seabed have been proposed and are being used in various areas. However, the

---
[1)] Ph. D. Candidate
[2)] Professor

possibility and economic feasibility of constructing the subsea tunnel or immersed tunnel are greatly affected by the seabed. If the depth of the seabed is too deep, the tunnel cannot be immersed, or it takes too much cost, and when a dangerous situation in the ground, such as an earthquake, a problem may occur in the stability of the tunnels (Jiang et al., 2018). As an alternative, a submerged floating tunnel (SFT) has been proposed (Martinelli et al., 2010). The SFT is operated fixed by a buoyant tunnel in a specific depth of water by methods such as pontoon and tether (Won and Kim, 2018). It is less affected by the weather environment above the water surface or by waves, and it is comparatively free from the influence of ground motion (Mazzoloani et al., 2008). However, to provide a path between lands through water, the SFT must be connected to the ground. As the SFT is connected to the ground, the tunnels are distinguished as the bored tunnel in ground and the SFT in the water. They have different constraint conditions, and the risk of stress concentration in the shore connection is an essential issue for the SFT design (Kang et al., 2020).

The previous study related to the SFT has focused only on the hydro-dynamic behavior of the SFT (Hong and Ge, 2010; Jin and Kim, 2021), and few studies considered the shore connection. Kang et al. (2020) conducted a numerical analysis to evaluate the stress concentration at the shore connection in the static condition. They found that the shore connection with the soft joint can release the stress concentration. Also, the study suggested that the grouting material with low stiffness can absorb the displacement transferred from the SFT, causing the stress to be distributed into the grouted layer rather than concentrated at the shore connection. This previous study shows that allowing displacement at the boundary between the bored tunnel and the SFT would be a stable design; however, consideration for the dynamic behavior is not included. To evaluate the stability of SFT, analysis relevant to its dynamic behavior due to the current and tidal loads is necessary (Jin et al., 2020).

Therefore, this study aims to conduct a numerical analysis to evaluate the effect of shore connection design under the dynamic loading condition. When the dynamic load is applied on the SFT, and the SFT behaves dynamically, the stress and strain that occurred in the bored tunnel, shore connection, and surrounding ground were observed. The numerical simulations with various shore connection types were conducted to understand the effect of shore connection stiffness in the dynamic condition.

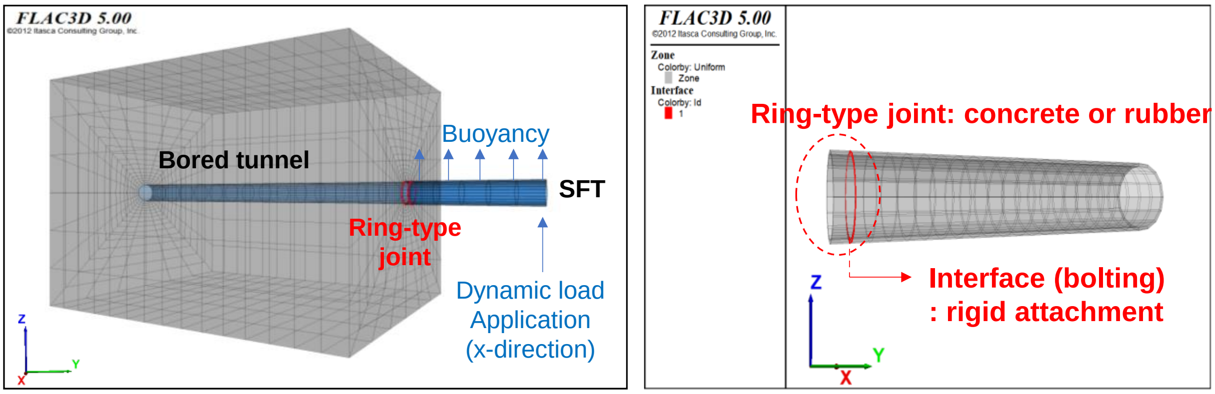

Fig. 1 Numerical model for the shore connection of SFT

2. NUMERICAL METHODOLOGY

The shore connection of SFT was simulated with a three-dimensional numerical model, including several assumptions for simplifying the situation. The numerical model was formed with commercial software, Fast Lagrangian Analysis of Continua in 3-Dimension (FLAC 3D), based on the finite difference method. To simplify the situation simulated in the numerical analysis, only a single segment of SFT was formed.

2.1 Numerical model

The numerical model simulates a single span of SFT, shore connection, bored tunnel, and ground (Fig. 1). The ground was formed with the Mohr-Coulomb model for simulating the elastoplastic behavior of granite. The tunnels, including the connection, were formed with the linear elastic model to represent the elastic behavior of concrete. The properties of each element were assumed as the general material characteristics, as shown in Table 1 and Table 2. The shore connection was constructed in the form of a ring-type joint with a length of 0.5 cm, and the numerical cases were performed by diversifying its properties from concrete to reinforce rubber.

Table 1 Properties for ground

Type	Value
Rock type	Granite
Constitutive model	Mohr-Coulomb
Density [kg/m^3]	2700
Elastic modulus [GPa]	40
Shear modulus [GPa]	16
Bulk modulus [GPa]	26.7
Friction angle [degrees]	30
Cohesion [MPa]	10
Tensile strength [MPa]	16

Table 2 Properties for tunnels

Type	Value
Tunnel material	Concrete
Constitutive model	Linear elastic
Tunnel diameter [m]	23
Elastic modulus [GPa]	30
Material density [kg/m^3]	3000
Segment thickness [m]	1.0
Segment length [m]	50

2.2 Numerical Analysis procedure

Assumptions for environments The numerical analysis was conducted under various environmental conditions to secure reliability. The SFT and its shore connection are affected by both the marine and geotechnical environments. To consider the marine environment, the hydrostatic pressure acting on the surface of SFT, the buoyancy acting on the SFT body, and a dynamic force acting on the end of SFT were simulated. The pressures were derived by assuming that the shore connection is placed at a depth of 61.5 m, buoyancy-weight ratio (BRW) is 1.38, and hydrostatic pressure is 620 kPa based on the previous study (Jin and Kim, 2017). The dynamic load applied on the end of SFT, which represent the tidal and current acting on the whole SFTs, was assumed as a sinusoidal wave with an amplitude of 26 MN and loading frequency of 2 Hz. To consider the geotechnical environmental condition, soil-tunnel interaction for the bored tunnel and soil damping characteristics were simulated. The soil-tunnel interaction was applied by the interface properties, providing the coupling stiffness as:

$$k_{coupling} = \max[\frac{K + \frac{4}{3}G}{\Delta z_{\min}}], \tag{1}$$

where K is the bulk modulus, G is the shear modulus, and Δz_{min} is the smallest dimension of an adjoining zone at the interface (Itastca, 2013). The ground damping was inputted with the Hardin model (Hardin and Hilbe, 2014), adjusting the reference strain of 0.06.

Simulation steps In order to improve the validity of the numerical analysis, several preparatory steps were taken to create a proper stress state before the main analysis. First, static analysis was performed to simulate the stress conditions under gravitational and hydrostatic conditions by simulating the ground only before tunnel construction. After that, the numerical models for the underground bored tunnel and SFT were constructed. The environmental factors other than dynamic loads were considered through static analysis that reflected the tunnel's weight, water pressure acting on the tunnel, and buoyancy. As a final step, the behavior of the tunnel and the ground was evaluated while applying a dynamic load to the statically equilibrated model.

Simulation cases The material of shore connection formed with a ring-type joint was considered as a variable in this numerical analysis. A typical tunnel-to-tunnel connection continuously connects the tunnel linings made of concrete without including a separate connecting body. In this study, the effect of shore connection on dynamic behavior was investigated by simulating the case for simulating the general case (i.e., concrete connection) and the four other cases where the shore connection was made of reinforced rubber. The properties of shore connection for each case are summarized in Table 3. In each case, all other conditions except the shore connection property were identical. Both the behavior of shore connection in static equilibrium without dynamic load and the behavior of shore connection under dynamic load were observed, and the effect of shore connection property was analyzed by comparing the results.

Table 3 Numerical cases

Shore connection	Elastic stiffness	Poisson's ratio
Concrete	30.0 GPa	0.15
Rubber 1	3.19 MPa	0.45
Rubber 2	6.38 MPa	0.45
Rubber 3	12.76 MPa	0.45
Rubber 4	25.52 MPa	0.45

3. RESULT AND DISCUSSION

3.1 Static analysis

The numerical results from the static analysis showed that the static equilibrium is reached when the SFT weight and the buoyancy applied on the SFT are balanced. The amplitude of the buoyancy is larger than the weight due to the BWR that is larger than 1.0; thus the SFT moved upward, causing stress in the shore connection and ground. The shore connection serves to hold the SFT so that it does not deviate from the target depth. The stress distributions of shore connection after the static equilibrium state are shown in Fig. 2. As the SFT floats upward by buoyancy, stress occurs in the shore connection, which is constrained by the ground and the bored tunnel. The connection with stiffer material caused more considerable stress at the bottom. When the reinforced rubber with relatively low stiffness is installed, the stress caused by SFT displacement was not concentrated at the shore connection, and it was transferred to the surrounding ground or bored tunnel. This result shows remarkable similarity to the results of a previous study (Kang et al., 2020).

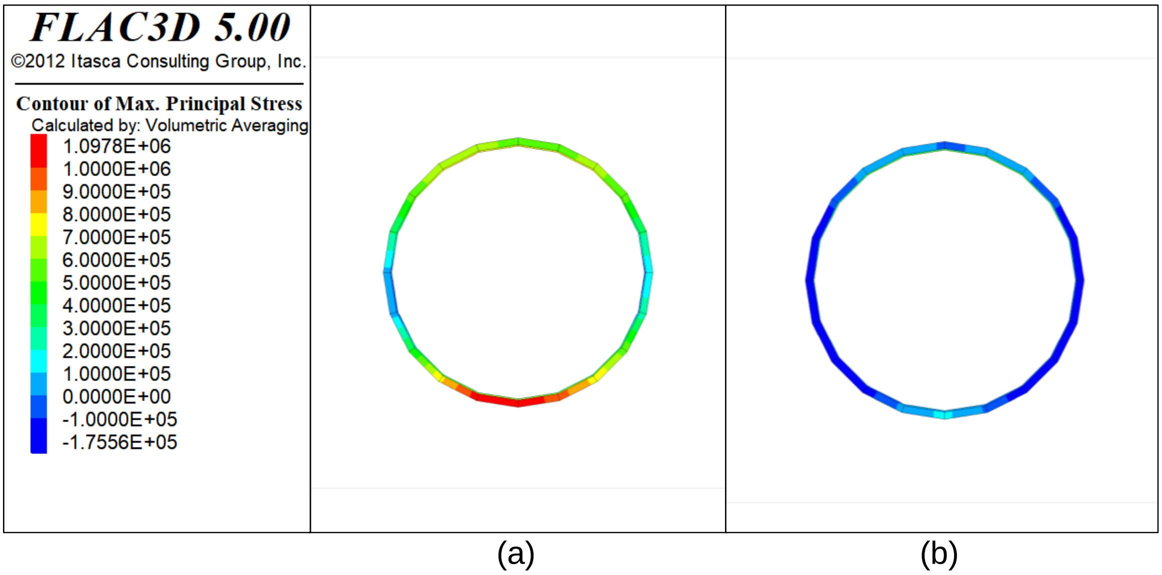

Fig. 2 Stress distribution in the shore connection with (a) concrete and (b) reinforced rubber as the result of static analysis

3.2 Dynamic analysis

The dynamic analysis was conducted after the static analysis, which includes the statically equilibrated stress state, by additionally applying a dynamic load at the end of SFT in the lateral direction. To investigate the dynamic analysis results only, the displacement that occurred during static analysis was initialized as 0, and the direction of the dynamic load was determined as the lateral direction. The dynamic load was applied for 5 seconds, and the analysis results were evaluated based on the peak point at the last cycle of loading. The SFT, bored tunnel, shore connection, and surrounding ground were observed in terms of the distribution of strain or stress.

Submerged floating tunnel The SFT behaves with very little restraint pressure. Since it is composed of a perfectly elastic body, a dynamic behavior similar to the input dynamic load was observed as shown in Fig. 3. Since the dynamic load was applied at the end of SFT, the displacement observed at the end is the largest. The displacement decreases as the observing point approach the shore connection. As the soft shore connection was used, the displacement of SFT near the shore connection increased as shown in Fig. 4. Compared to the case of the concrete joint, the maximum displacement increases by seven times when the soft rubber joint is used. This result implies that the maximum displacement is dominantly controlled by the shore connection stiffness, which can be considered a boundary condition. Therefore, the design for shore connection must include the consideration related to the resonance. As the shore connection becomes stiffer, the resonant frequency of SFT decreases (Park et al., 2022). Generally, the resonant frequency of the SFT is much larger than the loading frequency of tidal or current loads. However, if the resonant frequency decreases with the soft shore connection, the increased displacement of SFT can redound a significant risk on excessive displacement with the resonance.

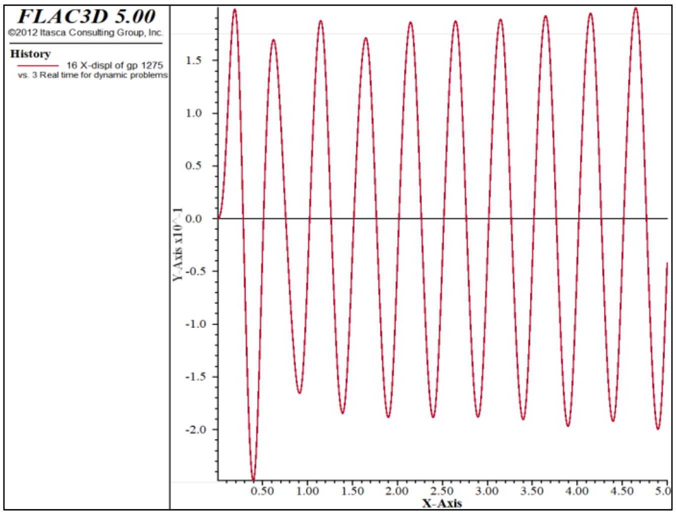

Fig. 3 Lateral displacement of the SFT

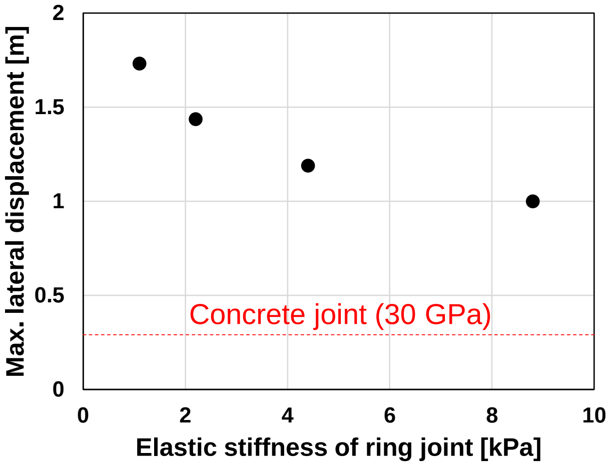

Fig. 4 Maximum displacement of SFT at the end according to shore connections

<u>Shore connection</u> As the lateral cyclic load was applied, the shore connection exhibits stress concentrations according to the lateral displacement of SFT (Fig. 5). As the shore connection is made of a weaker material, the displacement of the overall shore connection and SFT increases. However, the magnitude of the distributed stress decreases and the stress concentration is resolved. This tendency is similar to those from the static analysis. However, since the resonance and displacement levels are taken very seriously in the dynamic condition, the optimal shore connection stiffness needs to be determined considering the dynamic characteristics of the whole system, including ground, shore connection, and SFT. Considering only the shore connection, if it is made of a soft material, the stress is reduced, but the displacement is significantly increased. Therefore, it is expected that it will be appropriate to keep the stiffness of the material sufficiently high and to satisfy the allowable displacement.

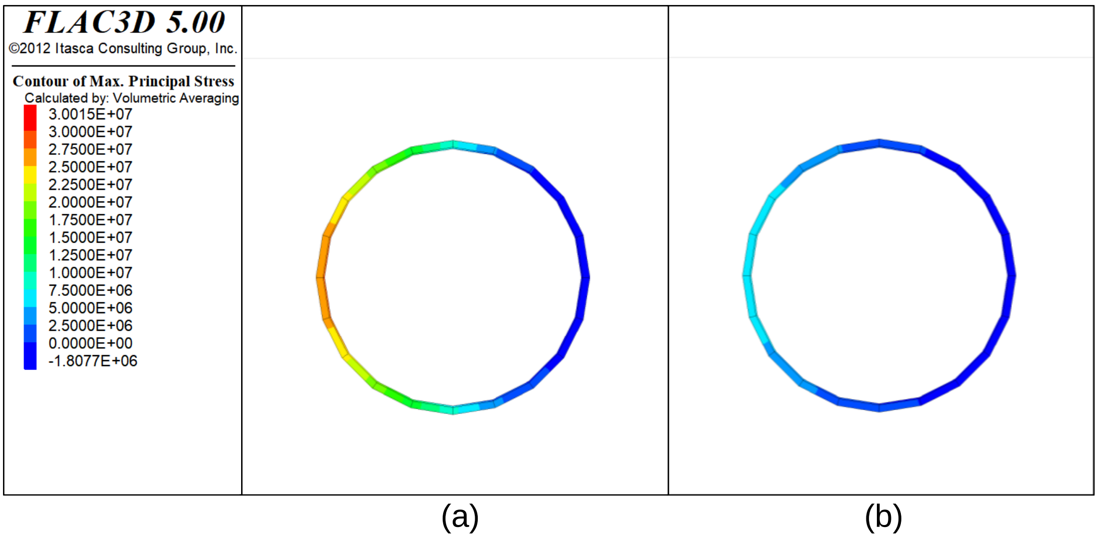

Fig. 5 Stress distribution in the shore connection made by (a) concrete and (b) rubber as the result of dynamic analysis

Underground bored tunnel   The bored tunnel is loaded by the shore connection, which behaves due to the SFT. Therefore, the shore connection stiffness affects the characteristic of load transferred into the bored tunnel. As shown in the results presenting the principle (Fig. 6) and shear (Fig. 7) stresses distribution in the bored tunnel, the magnitude of the stress was not too large, considering the general expected strength of the concrete tunnel because the dynamic load applied on the SFT was assumed to be not very large. However, it is necessary to evaluate the stress distribution characteristics in the bored tunnel according to the shore connection design to prepare for the situation when a huge dynamic load is applied, such as an earthquake. The lower the shore connection stiffness, the lower the magnitude of the load transmitted to the bored tunnel. Even when no dynamic load is applied, earth pressure due to the weight of the surrounding soil acts on the bored tunnel. To evaluate the effect of the load transmitted from the SFT in more detail, the load acting on the crown and sidewall of the bored tunnel was observed (Fig. 8). As a result, the magnitude of the force applied to the crown part of the bored tunnel, which moved in the lateral direction, did not differ significantly from the magnitude of the earth pressure.

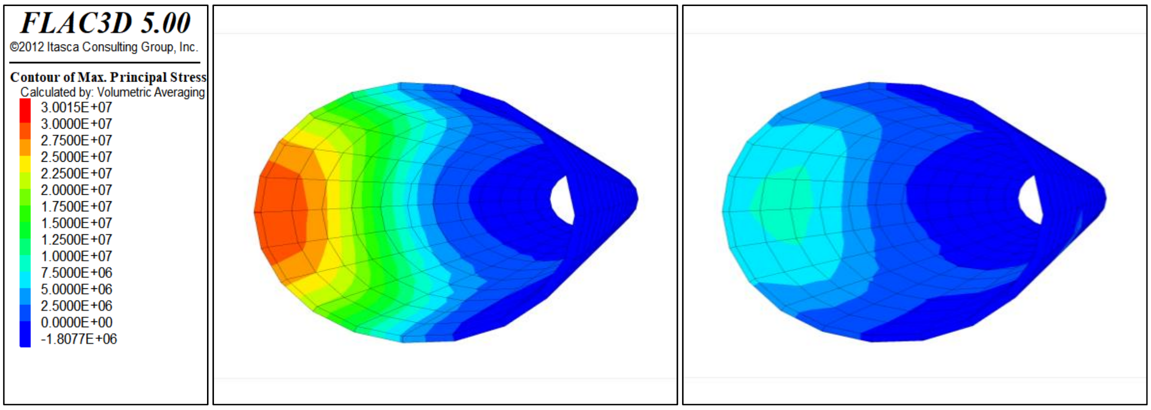

(a) (b)

Fig. 6 Stress distribution in the bored tunnel in cases with (a) concrete and (b) rubber

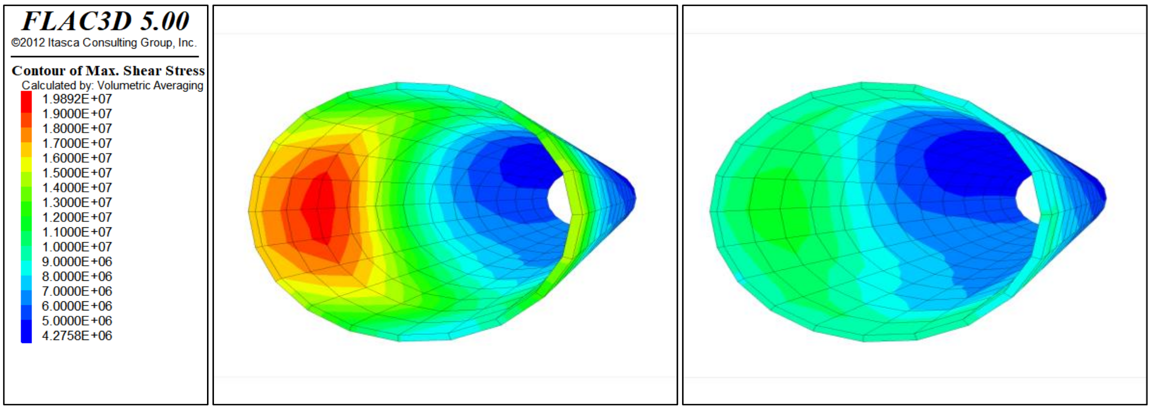

(a) (b)

Fig. 7 Shear stress distribution in the bored tunnel with shore connection made of (a) concrete and (b) rubber

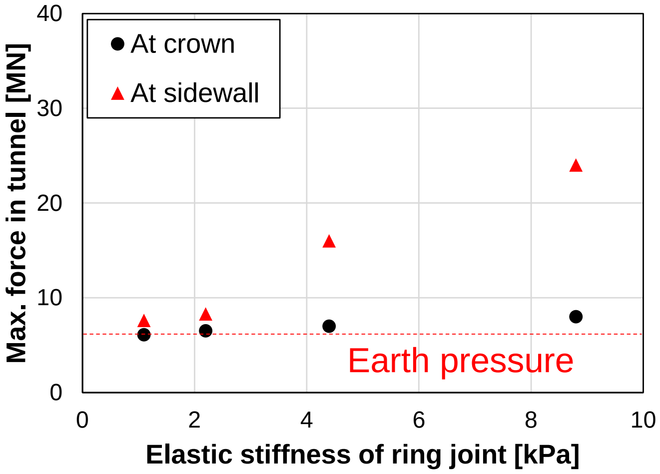

Fig. 8 Maximum force applied at the crown and sidewall of the bored tunnel with various shore connection stiffness

This result indicates that the shear stress increase due to the lateral motion is not significant. On the other hand, the magnitude of the force acting on the sidewall increased with a large difference as the stiffness of the ring-type joint increased. Therefore, in order to consider the stability of the bored tunnel, it is necessary to understand the behavior of the tunnel and the ground. Additionally, it is important to determine the dangerous part according to the direction of the applied load and the appropriate determination of the stiffness of the ring joint of the shore connection.

<u>Ground surrounding shore connection</u> The ground surrounding shore connection experiences continuous deformation according to the dynamic behavior of SFT. Since the ground model was constructed with the elastoplastic model, the plastic strain

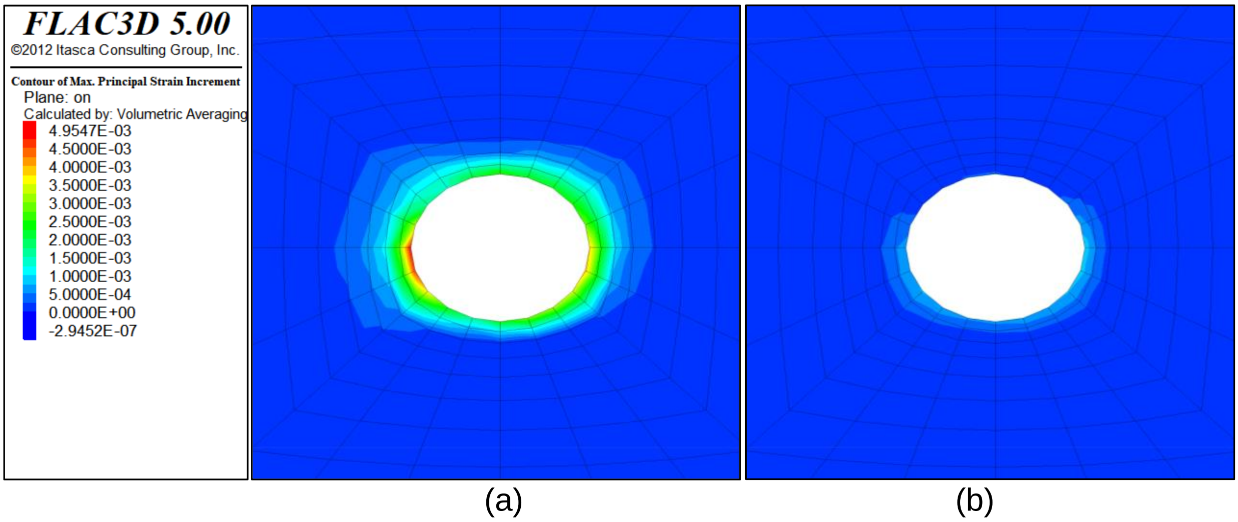

Fig. 9 Strain distribution in the ground surrounding shore connection with the shore connection made of (a) concrete and (b) rubber

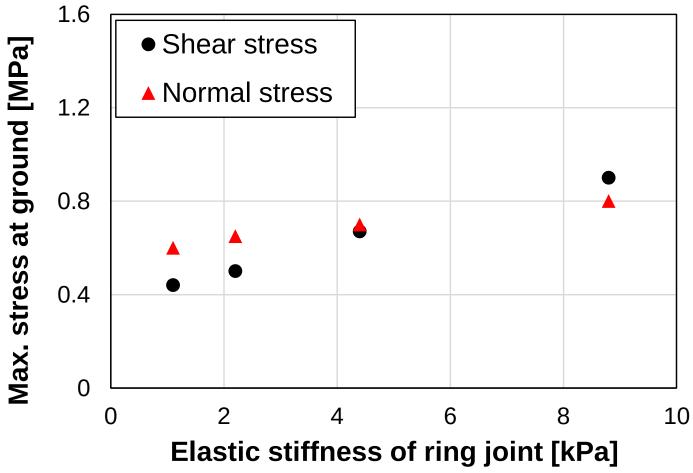

Fig. 10 Normal and shear stresses occurred in the ground surrounding shore connection with various shore connection stiffness

occurred during the dynamic behavior needs to be considered. As the concrete joint was installed as the shore connection, the stress transferred to the ground was significant, causing considerable strain as shown in Fig. 9(a). Using the soft shore connection, the strain occurring in the ground was significantly decreased as shown in Fig. 9(b). Observing the shear and normal stresses in the ground, the stresses increased as the stiffer joint was used for the shore connection. Contrary to the results obtained in the bored tunnel, the increase in shear stress according to the increase in shore connection stiffness was greater than that of normal stress (Fig. 10). When the softer shore connection was used, the shear stress was smaller than normal stress, similar to the results observed in the bored tunnel. It is expected that the strain in the normal direction increased according to the repeated dynamic load, and as a result, the maximum normal stress became smaller than the maximum shear stress.

4. CONCLUSIONS

In this study, the SFT and shore connection were simulated using a numerical method, and behavioral characteristics according to the stiffness of the shore connection in static and dynamic conditions were analyzed. The results of the static analysis performed before the dynamic analysis showed a similar tendency to the existing literature, and showed that the low-stiffness shore connection could improve the stability by relieving the stress concentration. However, when considering the behavior of the SFT as well as the shore connection under the dynamic load condition, it was confirmed that the soft shore connection has the potential to cause excessive displacement amplification. It was confirmed that the dynamic load transferred to the bored tunnel decreased as the stiffness of the shore connection decreased, and the effect of the load was applied to the tunnel as normal stress rather than shear stress. As a result of observing the strain and stress distributed in the ground surrounding shore connection, it was confirmed that the magnitude of the stress in the shear direction may be larger than that of normal when plastic strain occurs due to the continuous dynamic load. Considering the overall results, when a shore connection is constructed using a joint with low stiffness, the deformation of the shore connection increases and the magnitude of the stress acting on the surrounding tunnels and ground decreases. However, it seems that the direction, magnitude, and frequency of the dynamic load should all be considered mainly to design the shore connection of the SFT. The shore connection stiffness or grouting material can be determined by predicting the degree of plastic deformation of the ground according to the loading direction and the magnitude of dynamic load. The shore design that can prevent the resonance of the SFT should be devised in consideration of the loading frequency. The results of this study are expected to be able to contribute when conducting detailed research on a specific site in the future by preliminary reviewing matters to be considered carefully in shore connection design.

ACKNOWLEDGEMENT

This work was supported by UNDERGROUND CITY OF THE FUTURE program funded by the Ministry of Science and ICT and the National Research Foundation of Korea (NRF) grant funded by the Korea government (MSIT) (No. 2017R1A5A1014883).

REFERENCES

Hardin, James W. and Joseph M. Hilbe. (2014), "Generalized estimating equations: Introduction." *Wiley StatsRef: Statistics Reference Online*.

Hong, Y. and Ge, F. (2010), “Dynamic response and structural integrity of submerged floating tunnel due to hydrodynamic load and accidental load”. *Procedia Engineering*, **4**, 35-50.

Itasca, F. D. (2013), “Fast lagrangian analysis of continua in 3 dimensions”. Online Manual, 175-180.

Jiang, B., Liang, B., and Wu, S. (2018), “Feasibility study on the submerged floating tunnel in Qiongzhou strait, China”. *Polish Maritime Research*.

Jin, C. and Kim, M. (2021), “The Effect of Key Design Parameters on the Global Performance of Submerged Floating Tunnel under Target Wave and Earthquake Excitations”. *CMES-Computer Modeling in Engineering and Science*, **128**, 315-337.

Jin, R., Gou, Y., Geng, B., Zhang, H. and Liu, Y. (2020), “Coupled dynamic analysis for wave action on a tension leg-type submerged floating tunnel in time domain”. *Ocean Engineering*, **212**, 107600.

Jin, C. and Kim, M. (2017), “Dynamic and structural responses of a submerged floating tunnel under extreme wave conditions”. *Ocean Systems Engineering*, **7**(4), 413-433.

Kang, S.-J., Kim, J.-T. and Cho, G.-C. (2020), “Preliminary study on the ground behavior at shore connection of submerged floating tunnel using numerical analysis”. *Geomech. Eng.*, **21**, 133-142.

Martinelli, L., Barbella, G. and Feriani, A. (2010), “Modeling of Qiandao Lake submerged floating tunnel subject to multi-support seismic input”. *Procedia Engineering*, **4**, 311-318.

Park, J., Kang, S. J., Hwang, H. J. and Cho, G. C. (2022), “Numerical study on the resonance behavior of submerged floating tunnels with elastic joint”. *Geomechanics and Engineering*, **29**(3), 207-218.

Won, D. and Kim, S. (2018), “Feasibility study of submerged floating tunnels moored by an inclined tendon system”. *International Journal of Steel Structures*, **18**(4), 1191-1199.

Xiao, J. and Huang. G. (2010), "Transverse earthquake response and design analysis of submerged floating tunnels with various shore connections". *Procedia Engineering*, **4**, 233-242.